Water vapor imaging in the troposphere by combination of GNSS occultation data and ground-based GPS measurements

Ulrich Foelsche and Gottfried Kirchengast

Institute for Geophysics, Astrophysics, and Meteorology, University of Graz (IGAM/UG), Universitaetsplatz 5, A-8010 Graz, Austria

phone: +43 316 380 8590, fax: +43 316 380 9825, email: ulrich.foelsche@kfunigraz.ac.at

Introduction

The potential of Global Positioning System (GPS) measurements for accurately estimating vertically and slant-path integrated water vapor between GPS satellites and ground-based receivers has been demonstrated recently (e.g., [1],[2],[3]).

Global Navigation Satellite System (GNSS) based radio occultation, on the other hand, has been shown to deliver accurate near-vertical profiles of atmospheric variables such as temperature and humidity with high vertical resolution (e.g., [4]). Height resolving imaging of atmospheric water vapor becomes feasible when occultation profiles from spaceborne receivers in Low Earth Orbits (LEO) are combined with ground-based GNSS data from a co-located receiver network.

Methods

We developed a two-dimensional, height-resolving tomographic imaging technique following the Bayesian approach for optimal combination of information from different sources.

The reconstruction plane, defined by the occultation rays, is divided into picture elements (pixels) with assumed constant water vapor density (see Fig. 1). For the ground measurements, the rays can be considered as straight lines (the integrals in the forward problem degenerate into simple sums of densities times ray lengths in each pixel), but for the occultation rays bending cannot be neglected. The latter are thus not incorporated directly into the inversion, but as "a priori" information via optimal estimation [5], exploiting that the occultation delivers a reliable mean refractivity profile. The corresponding mean water vapor density profile (representative for the entire retrieval domain) can be computed given additional temperature profile information (e.g., from the latest ECMWF analysis). The accurately measured vertical integrated water vapor (IWV) can be used to adjust the water vapor density profile to match in integral this IWV value (see Fig. 5d).

We show representative results, using simulated GNSS-based water vapor measurements from LEO and ground, derived from simple synthetic refractivity fields (Figs. 3 and 4) and from a realistic refractivity field based on a European Centre for Medium-range Weather Forecasts (ECMWF) analysis (Fig. 5).

Forward model scheme

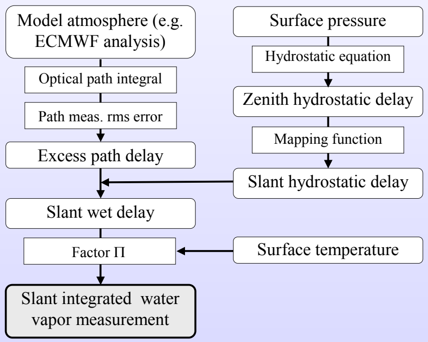

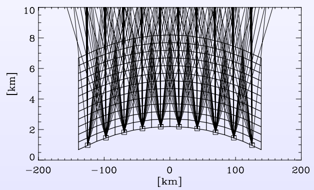

Fig. 1: Pixel geometry (ECMWF fields) and rays from 24 satellite positions (3 GNSS satellites, 8 positions per satellite during a 30 min interval) to 10 ground stations (indicated by squares). A total of 226 rays is shown, as only rays, that do not leave the reconstruction field sideward were used for the retrieval. The most slant rays are at 7° elevation (note the plot aspect ratio of ~ 1:22).

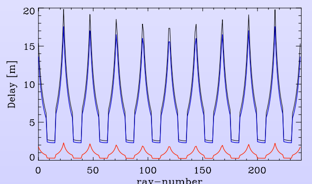

Fig. 2: Excess path delay (black), slant hydrostatic delay (blue) and wet delay (red) for a refractivity field located in Florida (centered at 27°N, 80°W). Each bundle of 24 ray-numbers corresponds to ray-paths between the different satellite positions and one ground station.

Tomographic scheme

$$\mathbf{y} = \mathbf{A}\cdot\mathbf{x} + \boldsymbol{\varepsilon}$$

$\mathbf{y}$ = measurement vector (slant integrated water vapor)
$\mathbf{A}$= design matrix (ray-path lengths within pixels)
$\mathbf{x}$ = state vector (water vapor densities within pixels)
$\boldsymbol{\varepsilon}$ = measurement error vector

Retrieval scheme

$$\mathbf{x}_{retr} = \mathbf{x}_{ap} + \mathbf{S}_{retr}\mathbf{A}^T\mathbf{S}_{\varepsilon}^{-1}(\mathbf{y} - \mathbf{A}\mathbf{x}_{ap})$$

$$\mathbf{S}_{retr} = (\mathbf{A}^T\mathbf{S}_{\varepsilon}^{-1}\mathbf{A} + \mathbf{S}_{ap}^{-1})^{-1}$$

$\mathbf{x}_{retr}$ = retrieved state vector
$\mathbf{x}_{ap}$ = *a priori* state vector (occultation-derived)
$\mathbf{S}_{retr}$ = retrieval covariance matrix
$\mathbf{S}_{\varepsilon}$ = measurement covariance matrix
$\mathbf{S}_{ap}$ = *a priori* covariance matrix

In order to basically investigate the performance of the retrieval algorithm, we directly used synthetic water vapor fields and corresponding SIWV values. The *a priori* field used in this case was simply the mean density profile extended over the entire reconstruction domain. The latitude range used was arbitrarily chosen centered at 45° (Figs. 3 and 4).

In the ECMWF case (Fig. 5) we used the full forward model scheme outlined.

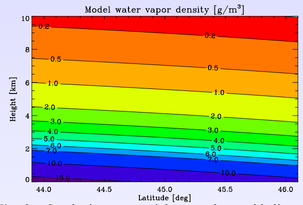

Fig. 3a: Synthetic exponential atmosphere with linear horizontal gradient. The exponential decrease with height is described by a climatological (constant) water vapor scale height of 2 km.

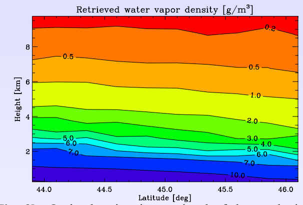

Fig. 3b: Optimal estimation retrieval of the synthetic exponential atmosphere with linear horizontal gradient, assuming an rms SIWV error of 1.5 kg/m². Retrieval height-domain 0 - 10 km, 20 x 10 pixels.

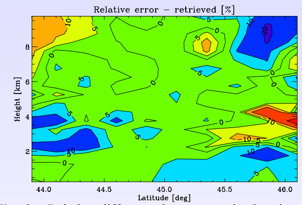

Fig. 3c: Relative difference between optimal estimation retrieval (Fig. 3b) and the original water vapor density field (Fig. 3a).

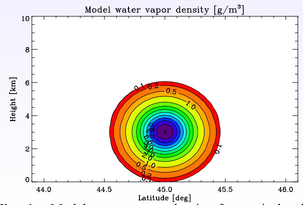

Fig. 4a: Model water vapor density for an isolated Gaussian blob with a vertical half-width of 1 km, and a horizontal half-width of 0.15° (~17 km).

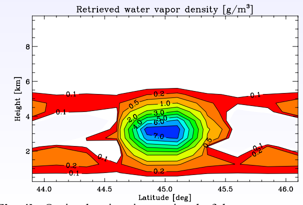

Fig. 4b: Optimal estimation retrieval of the water vapor density field shown in Fig. 4a, assuming an rms SIWV error of 1.5 kg/m².

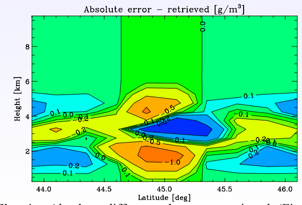

Fig. 4c: Absolute difference between retrieved (Fig. 4b) and model water vapor density (Fig. 4a), respectively, for the scenario of an isolated Gaussian blob.

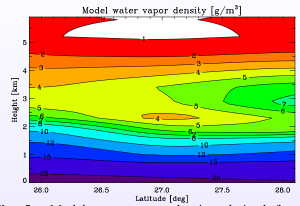

Fig. 5a: Model water vapor density, derived from ECMWF analysis data over Florida for October 20, 1995 (12 UT time layer, T213L31 resolution).

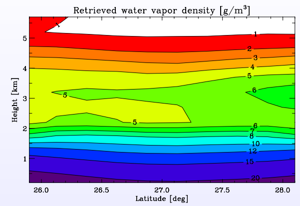

Fig. 5b: Optimal estimation retrieval of the water vapor density field shown in Fig. 5a (Florida case). Height range 0 - 6 km, 12 x 10 pixels (see Fig. 1).

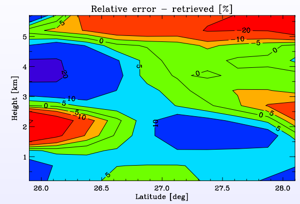

Fig. 5c: Relative difference between retrieved (Fig. 5b) and model water vapor density (Fig. 5a) - Florida case.

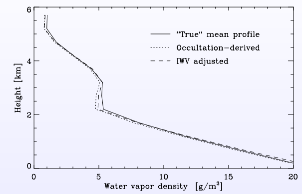

Fig. 5d: Averaged profile of the water vapor density field shown in Fig. 5a (solid line), density profile obtained by mimicked radio occultation (dotted), and occultation profile after IWV adjustment (dashed), the latter used as *a priori* profile.

Summary and conclusions

Tomographic imaging becomes feasible when ground-based measurements are combined with spaceborne measurements, which requires co-location of ground receivers and occultation events. We developed a technique for tropospheric water vapor imaging, where the ground-based line integral measurements are combined with an occultation profile employing optimal estimation. Instead of occultations also other profile data (e.g., from radiosondes) could be used.

The retrieval algorithm was tested by computing different scenarios with the aid of simulated data. We conclude that the presented retrieval algorithm is capable to reproduce realistic atmospheric features, like secondary water vapor maxima near the top of the tradewind inversion.

In areas with low absolute humidities, the occultation accuracy is significantly affected by the accuracy of the required *a priori* temperature profiles. A procedure like the mentioned IWV adjustment should be employed in this case in order to suppress biases. But even in areas with low absolute humidities, like in Finland, useful two-dimensional information can be obtained with the presented optimal estimation approach.

In areas with high absolute humidities, variations of the water vapor density are generally less pronounced, the occultation profile is less sensitive to errors in the *a priori* temperature profile, and the retrieval results are generally of good quality.

We are confident that the proposed methodology will find fruitful application to genuine data and thus contribute to the provision of much needed information on the regional and global water vapor distribution.

References

[1] T.R. Emardson et al., *J. Geophys. Res.*, 103, 1 807-1 820, 1998.
[2] J. Duan et al., *J. Appl. Met.*, 35, 830-838, 1996.
[3] R. Ware et al., *Geophys. Res. Lett.*, 24, 417-420, 1997.
[4] C. Rocken et al., *J. Geophys. Res.*, 102, 29 849-29 866, 1997.
[5] C.D. Rodgers, *J. Geophys. Res.*, 14, 609-624, 1976.

© 2000 by IGAM/UG